

All-Optical Flip-Flop Based on Coupled Laser Diodes

Martin T. Hill, *Associate Editor, IEEE*, H. de Waardt, G. D. Khoe, *Fellow, IEEE*, and H. J. S. Dorren

Abstract—An all-optical set–reset flip-flop is presented that is based on two coupled lasers with separate cavities and lasing at different wavelengths. The lasers are coupled so that lasing in one of the lasers quenches lasing in the other laser. The flip-flop state is determined by the laser that is currently lasing. A rate-equation based model for the flip-flop is developed and used to obtain steady-state characteristics. Important properties of the system, such as the minimum coupling between lasers and the optical power required for switching, are derived from the model. These properties are primarily dependent on the laser mirror reflectivity, the inter-laser coupling, and the power emitted from one of the component lasers, affording the designer great control over the flip-flop properties. The flip-flop is experimentally demonstrated with two lasers constructed from identical semiconductor optical amplifiers (SOAs) and fiber Bragg gratings of different wavelengths. Good agreement between the theory and experiment is obtained. Furthermore, switching over a wide range of input wavelengths is shown; however, increased switching power is required for wavelengths far from the SOA gain peak.

Index Terms—Flip-flop, memories, optical bistability, semiconductor lasers, semiconductor optical amplifiers.

I. INTRODUCTION

OPTICAL bistable and multistable devices based on laser diodes (LDs) have been extensively studied as they have many potential applications in optical computing and telecommunications. The most important types of optical bistable laser diode devices can be classified into three broad types: 1) absorptive bistability, involving multi-section LDs, in which a section acts as a saturable absorber; 2) two modes or polarization bistability, where the lasing mode suppresses the other mode via nonlinear gain effects; and 3) dispersive bistability, where the bistability is based on refractive index changes due to carrier-density changes in the LD. A review and explanation of these three types of bistable LDs can be found in [1].

The optical bistable system considered here is not based upon any of the above-mentioned effects. Rather, it is based on the fact that lasing at the natural lasing wavelength in a laser can be quenched when sufficient external light is injected into the laser cavity. The injected external light is not at the same wavelength as that of the lasing light. Lasing is stopped because the gain inside the laser drops below lasing threshold due to the amplified external light.

The optical flip-flop considered here consists of two coupled lasers (see Fig. 1). Laser 1 lases at wavelength λ_1 , and only λ_1

light from laser 1 is injected into laser 2. Laser 2 lases at wavelength λ_2 , and only λ_2 light from laser 2 is injected into laser 1. One laser acts as the master and suppresses lasing action in the other laser, which acts as a slave. The role of master and slave can be interchanged due to system symmetry. Thus, the system can be in one of two states, depending on which laser is lasing, and the state can be determined from the wavelength of the light output. The flip-flop is in state 1 if the output light has wavelength λ_1 is output, and state 2 if the output light has wavelength λ_2 . We have chosen to use wavelength to differentiate the lasers in the system. Furthermore, light emitted from the master laser flows all the way through the active region of the slave laser, without any light being reflected back into the master laser. In some implementations of the flip-flop, reflections of light back into the master could be significant and may be modeled according to [2]. However, the model and system behavior would be more complicated, and so is not considered here.

To change between states, light from outside the flip-flop can be injected into the master laser to stop or reduce its light output. The injected light is not at the lasing wavelength of the master laser and passes through the master laser. The reduction or absence of light from the master laser allows the slave laser to start lasing and become the master. The flip-flop remains in the new state after the external light is removed.

The concept of a bistable laser system based on gain quenching was first proposed in [3]. However, the concept was only experimentally demonstrated two decades later in pulsed operation with dye lasers [4]. In [5], a bistable laser system based on gain quenching was theoretically studied, and suggestions for an implementation using laser diodes were given. In [6], a device was demonstrated which was loosely based on the ideas presented in [3]. However, this device was not based on coupled separate lasing cavities. Furthermore, the device required saturable absorbers to change the lasing thresholds for the two lasing modes in the system.

An optical flip-flop based on gain quenching offers a number of advantages. It can provide high contrast ratios between states. There is no difference in the mechanisms that change from state 1 to state 2 and vice-versa, permitting symmetric set–reset operation. The wavelength range of the input light, and the choice of output wavelengths, can be quite large. As we will show in this paper, the flip-flop has controllable and predictable switching thresholds. The flip-flop is not tied to a specific structure or technology, and does not rely on second-order laser effects such as refractive index changes or nonlinear gain. Thus, the flip-flop can be implemented with a wide range of laser and interconnection types. For example, in [7], a flip-flop based on gain quenching was demonstrated using free-space optics and operating at wavelengths around 680 nm. However, the flip-flop

Manuscript received March 7, 2000; revised October 26, 2000. This work was supported by the Netherlands Organization for Scientific Research (NWO) under the NRC Photonics Grant.

The authors are with the Department of Electrical Engineering—EH 12.33, Eindhoven University of Technology, 5600 MB Eindhoven, The Netherlands.

Publisher Item Identifier S 0018-9197(01)01617-7.

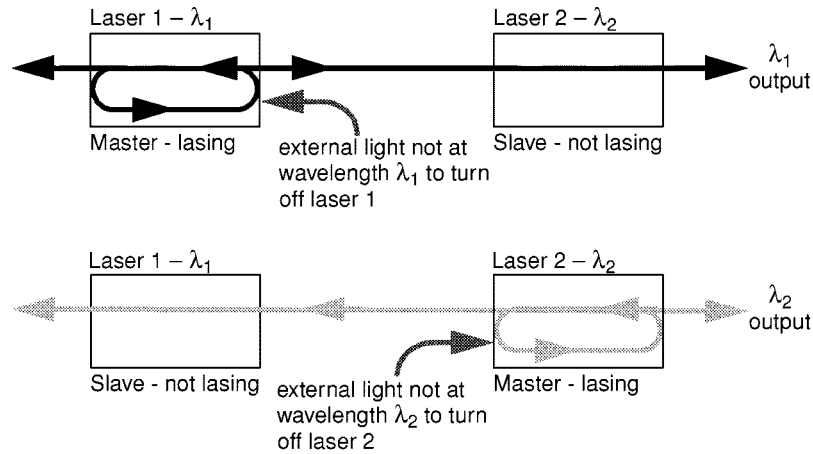


Fig. 1. Master-slave arrangement of two identical lasing cavities, showing the two possible states. In state 1, light from laser 1 suppresses lasing in laser 2. In state 2, light from laser 2 suppresses lasing in laser 1. To change states, lasing in the master is stopped by injecting light not at the master laser's lasing wavelength.

structure was not suitable for integration (as it used isolators). Furthermore, the free-space optic setup did not easily allow precise quantitative comparisons between theory and experiment.

In [7], the rate equation model used later in this paper was tersely presented (with a slight difference in the definition of one parameter and one rate equation). Here, we use the rate equation model as a base from which to derive a simplified model. Using the simplified model, the flip-flop operation is explained and important properties and results about the flip-flop are derived. Furthermore, the results from the model are later quantitatively compared with the experimental results.

Note that while the flip-flop does not rely on the effects of refractive index change and nonlinear gain, these effects will be present. Refractive index changes will cause changes in the wavelength of the lasers as the flip-flop switches state. Care should be taken to ensure that the wavelengths of the lasers are sufficiently different so that there is no overlap of the wavelengths during switching of states, and also that other effects such as four-wave mixing do not become significant. Non-linear gain effects may also affect the switching thresholds calculated here. The effects of refractive index change and nonlinear gain are not considered in this paper.

Furthermore, we have not considered thermal effects in the lasers due to power dissipation. However, for integrated flip-flops, this issue may need to be considered as at least two lasers will be operating on the same chip.

The rest of this paper is organized as follows. In Section II, we develop a model of the flip-flop using rate equations. In Sections II and III, we derive important properties of the flip-flop from the model. In Section IV, we experimentally demonstrate the system with lasers constructed from semiconductor optical amplifiers (SOAs) and fiber Bragg gratings (FBGs). Finally, the paper is concluded in Section V.

II. RATE EQUATION MODEL

We assume that each laser in the flip-flop (Fig. 1) consists of a gain section surrounded by two wavelength-dependent mirrors of reflectivity R at the lasing wavelength of the laser. For other

wavelengths, the mirror reflectivity is zero. We also assume that photons injected into the laser, by the other laser or an external source, pass through the wavelength-dependent mirrors of the laser. Furthermore, the photons pass through the gain section and are amplified just as would occur in a travelling-wave SOA.

The flip-flop is mathematically modeled using two coupled sets of rate equations (1) and (2) (where the indices used to describe laser 1 and 2 are $i = 1, 2$, and $j = 3 - i$). Each set describes one of the lasers. The number of photons S_i in the laser cavity at the lasing wavelength is given by (1), and the carrier number N_i in the laser cavity is given by (2)

$$\frac{dS_i}{dt} = \left(v_g G_i - \frac{1}{\tau_p} \right) S_i + \beta \frac{N_i}{\tau_e} \quad (1)$$

$$\frac{dN_i}{dt} = \frac{I}{q} - \frac{N_i}{\tau_e} - v_g G_i S_i - v_g G_i \zeta_i \left(\eta S_j \ln \left(\frac{1}{R} \right) + S_i^{\text{ext}} \right) \quad (2)$$

where

$$\zeta_i = \frac{e^{(G_i - \alpha_{\text{int}})L} - 1}{2L(G_i - \alpha_{\text{int}})} \quad (3)$$

$$G_i = \frac{\Gamma a}{V} (N_i - N_0) \quad (4)$$

$$S_i^{\text{ext}} = \frac{2L}{v_g} \frac{P_i^{\text{ext}}}{E}. \quad (5)$$

The photon lifetime τ_p is given by

$$\frac{1}{\tau_p} = v_g \left(\alpha_{\text{int}} + \frac{1}{L} \ln \left(\frac{1}{R} \right) \right). \quad (6)$$

In (2), S_i^{ext} represents the number of externally injected photons per laser cavity round-trip time ($2L/v_g$ s) and is used to change the flip-flop state. S_i^{ext} is related to the external power injected into the laser P_i^{ext} by (5). η is the fraction of photons leaving a facet of one of the lasers that are injected into the other laser. The light power at the lasing wavelength leaving a facet of one of

TABLE I
DESCRIPTION AND VALUE OF SYMBOLS USED IN EQUATIONS

Symbol	Description	Value
N_i	Carrier number in laser cavity i	
S_j	Photon number in laser cavity i	
S_i^{ext}	Photons from outside flip-flop injected into cavity i	
I	Injection current	89 mA
q	electronic charge	$1.6 \times 10^{-19} \text{C}$
v_g	group velocity in the active region	$8 \times 10^9 \text{ cm/s}$
a	gain factor	$2.9 \times 10^{-16} \text{ cm}^{-2}$
Γ	confinement factor	0.33
τ_e	carrier lifetime	1 ns
N_0	Carrier number for transparency	2.25×10^8
β	Spontaneous emission factor	5×10^{-5}
V	Volume of active region	$2.5 \times 10^{-10} \text{ cm}^3$
L	Length of active region	0.05 cm
α_{int}	internal losses	27 cm^{-1}
R	mirror reflectivity	0.04
η	coupling parameter	0.167
N_{th}	Threshold carrier number	
E	Photon Energy	

the lasers P_i is related to the photon number by the well-known equation [9]

$$P_i = E \frac{v_g}{2L} \ln\left(\frac{1}{R}\right) S_i. \quad (7)$$

Any symbols that are thus far unexplained, are described in Table I.

In the rate equation model, we have made the following assumptions.

- 1) Carrier concentration is assumed to be constant over the length of the cavity. This assumption allows the use of a simple SOA model [8] to model the laser gain section.
- 2) The effects of amplified spontaneous emission and residual facet reflectivities in [8] are ignored. These assumptions are valid for the typical gains required in the flip-flop and the quality of SOAs used in the experiments. In the experiments, the laser output power due to spontaneous emission was less than 4% of the output power at the lasing wavelength. Furthermore, the SOAs used had residual facet reflectivities approximately 400 times less than the mirror reflectivities used to form the lasers.
- 3) We assume that the differences between the wavelengths involved are only a small fraction of the wavelength they are centered around. Hence, we can simplify expressions by taking the energy of photons, at slightly different wavelengths, to be the same and equal to E .
- 4) The light injected into the laser experiences the same gain, guiding and internal loss as the light at the lasing wavelength inside the laser. Later, we will relax the assumption on the gain. These assumptions lead to simple analytic results and their accuracy is supported by experimental results.

A SOA model that assumes constant photon density and thus constant carrier concentration along the cavity length is given

in [8]. In (1) and (2), the only effect of injected photons is to reduce N_i via the right most term in (2). We have modeled the effect exactly as was done in [8], (taking into account our above assumptions on residual facet reflectivities and amplified spontaneous emission), and the right-most term in (2) is taken from [8] after converting from carrier and photon densities to carrier and photon numbers. The term in $\eta S_j \ln(1/R) + S_i^{\text{ext}}$ (2) represents the number of photons injected into the SOA in the period of $2L/v_g$ s by the other laser and an external source. These photon numbers are related to the power injected into the SOA by (5) and (7).

The essential difference in the rate equations presented here from those given in [5] is that, in [5], Γ and α_{int} are not taken into account when modeling the effect of injected light, whereas in the model of [8] they are. For the special case of $\Gamma = 1$ and $\alpha_{\text{int}} = 0$, the models are identical. However, the models diverge dramatically when $\Gamma \neq 1$ and $\alpha_{\text{int}} \neq 0$, due to the fact that Γ and α_{int} appear in an exponent (3). Furthermore, by including Γ and α_{int} in the model, simplified expressions for laser coupling and switching power are obtained.

The steady-state solution of the rate equations for a single laser can be found by setting the left-hand side of (1) and (2) equal to zero and solving for N_i and S_i . The steady-state solution can also be found for various values of injected external light S_i^{ext} , (taking $S_j = 0$ for the moment). A plot of the steady state N_i and S_i versus S_i^{ext} is shown in Fig. 2. It can be seen from Fig. 2 that S_i initially decreases linearly, while N_i remains approximately constant at the threshold level N_{th} . Assuming $N_i = N_{\text{th}}$, the slope of S_i in this initial linear section can be found from (2) to be $-\zeta_i$ for $N_i = N_{\text{th}}$. We denote the value of ζ_i when $N_i = N_{\text{th}}$ as ζ_{th} . N_{th} can be found from (1) and (4) by equating optical loss and gain [9] ($v_g G_i = 1/\tau_p$) to be

$$N_{\text{th}} = \frac{V}{\tau_p \Gamma v_g a} + N_0. \quad (8)$$

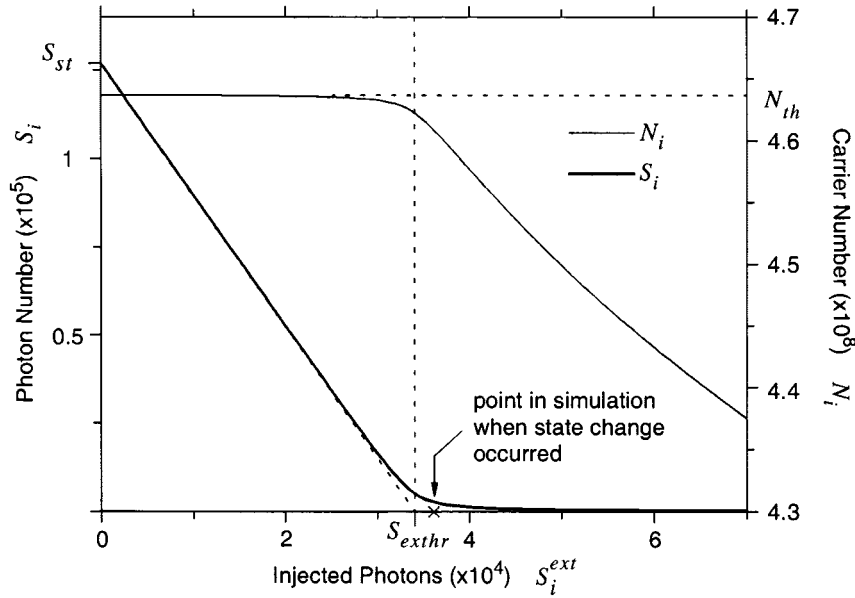


Fig. 2. Steady-state photon and carrier numbers of single laser versus injected photons.

From (3), (4), (6), and (8), ζ_{th} can be found to be

$$\zeta_{th} = \frac{(1/R) - 1}{2 \ln(1/R)}. \quad (9)$$

The photon number in the absence of external light injected into the laser is denoted by S_{st} , and from (1) and (2), it is found to be

$$S_{st} = \tau_p \left(\frac{I}{q} - \frac{N_{th}}{\tau_e} \right). \quad (10)$$

If the initial linear behavior of the laser is extended to the x axis of Fig. 2, then the value of S_i^{ext} at which it crosses the x axis is S_{extthr} and this value is found to be

$$S_{extthr} = S_{st}/\zeta_{th}. \quad (11)$$

Analytic approximations for N_i and S_i after light injection exceeds S_{extthr} can be found. However, they are not simple expressions, nor do we make particular use of them. The essential features of S_i after light injection exceeds S_{extthr} can be seen in Fig. 2. After S_i^{ext} exceeds S_{extthr} , S_i becomes asymptotic with the $S_i = 0$ axis and, thus, the slope of S_i , that is dS_i/dS_i^{ext} , approaches zero as S_i^{ext} is increased above S_{extthr} .

Considering the flip-flop system without any external influences, that is S_i^{ext} is set to zero, and the only light injected is from the other laser $\eta S_j \ln(1/R)$. A curve similar to that of Fig. 2 can be plotted but now with S_j versus S_i .

N_i and S_i can be considered as state variables of the flip-flop because the set of four variables describe a unique operating point or state of the flip-flop. We are particularly interested in the N_i, S_i , which satisfy the rate equations for the steady state. The steady-state solutions of the four rate equations can be found from the intersection points of the curves S_1 versus S_2 and S_2 versus S_1 just described in the preceding paragraph (see Fig. 3).

If the coupling parameter η between the lasers is high enough to allow the slope of the linear regions in Fig. 3 to be greater than

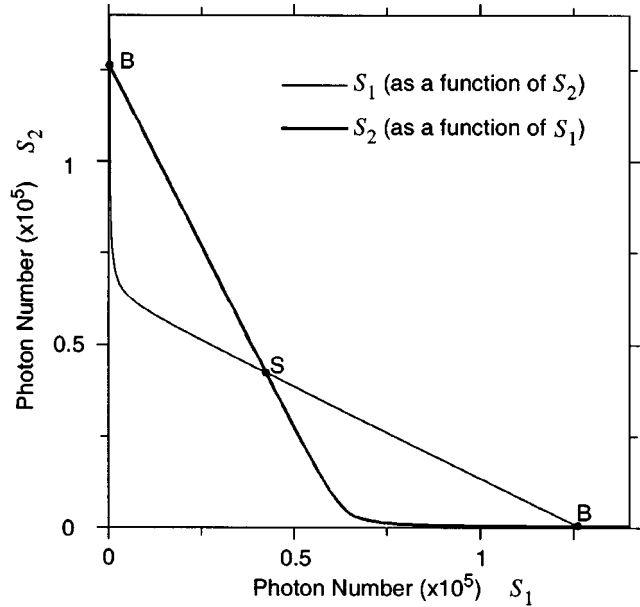


Fig. 3. Steady-state curves for the two lasers showing possible operating points.

one, then the curves will intersect at three points. The requirement on η for intersection at three points is found from (2) and (9) to be

$$\eta > \frac{2R}{1-R}. \quad (12)$$

Two of the intersection points (labeled B in Fig. 3) represent steady states with only one of the lasers above threshold. The other point (labeled S in Fig. 3) represents a symmetric state with both lasers lasing and at the same power. If the coupling is weak, that is η does not satisfy (12), then the curves will only intersect at one point, leading to only one possible symmetric state.

The maximum value of η (without amplification of photons travelling between the lasers) is one. From (12), the maximum

value of R for intersection at three points and, hence, possible bistable operation is $R = 1/3$. This medium value for R indicates it may not be possible to use all types of semiconductor lasers. Specifically, devices with high R such as VCSELs (vertical cavity surface emitting lasers), which benefit from low threshold currents and small cavity size, may not be suitable.

III. STEADY-STATE BEHAVIOR AND STABILITY

The steady-state solutions of the rate equations which represent stable states can be found by linearizing the flip-flop system [10] at a particular steady-state solution denoted by N_i^0, S_i^0 . In a small neighborhood around N_i^0, S_i^0 , the flip-flop, which is a nonlinear system, behaves like a linear system. The linearized system can be checked for stability using standard techniques [10] to determine the flip-flop stability for N_i^0, S_i^0 . However, this formal approach does not yield simple analytic expressions for crucial flip-flop properties in terms of the flip-flop parameters. Nor does it offer insight into how the flip-flop operates.

To obtain simple analytic expressions and more insight into the flip-flop behavior, we employ a simplified model. In the model, the lasers are represented by their steady-state photon number versus injected photon number curves (see Figs. 2 and 3). Also in the simplified model, the light output of the laser changes instantaneously in accordance with the input light. A time delay of $T/2$ s is experienced by light travelling between the lasers. In this simplified model, there are just two state variables: S_1 and S_2 .

In a small neighborhood around the steady-state values, we can linearize the laser steady-state characteristics used in the simplified model. Furthermore, we can consider the flip-flop to be a linear closed-loop control system with, for example, the photon number S_1 as the controlled quantity. The characteristic equation [10] of the closed-loop control system can be found to be

$$1 - hc^{-Ts} = 0 \quad (13)$$

where h is the gain around the loop for S_1

$$h = \left. \frac{dS_2}{dS_1} \right|_{S_1=S_1^0} \times \left. \frac{dS_1}{dS_2} \right|_{S_2=S_2^0}. \quad (14)$$

The particular values on the right-hand side of (14) depend on the operating point of each laser. For example, with the flip-flop in state 2, S_1 is small and laser 2 operates in the initial linear region of the steady-state characteristic (Fig. 2), so

$$\left. \frac{dS_2}{dS_1} \right|_{S_1=S_1^0} = -\eta \ln\left(\frac{1}{R}\right) \zeta_{\text{th}} = -\eta \frac{(1-R)}{2R}. \quad (15)$$

Furthermore, S_2 is large and laser 1 does not operate in the initial linear region, and, as mentioned in Section II, the value of dS_1/dS_2 will be close to zero.

For the flip-flop to be stable, the roots of the characteristic equations (13) must lie in the left half of the s plane [10]. That is, the real part of the roots are less than zero. By using a method to obtain the roots of the characteristic equation given in [11], the flip-flop is stable, provided that

$$-1 < h < 1. \quad (16)$$

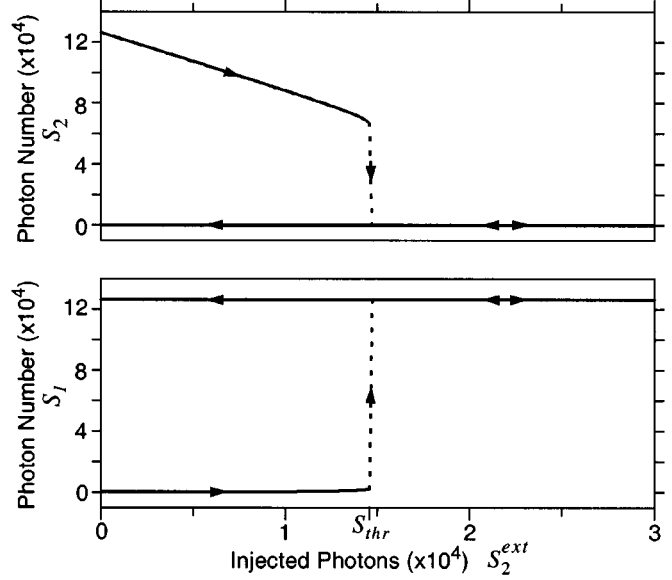


Fig. 4. Laser 1 and 2 photon numbers S_1, S_2 versus external light injected into laser 2 S_2^{ext} . Note that when the flip-flop is in state 2, S_2 is reduced as S_2^{ext} is increased toward S_{thr} , while at the same time S_1 remains approximately constant and close to zero. When S_2 is reduced to a level such that laser 1 is no longer forced below threshold the flip-flop switches state, with S_1 suddenly increasing and S_2 suddenly dropping to zero.

We can identify two general regimes where condition (16) is satisfied.

Firstly, when the flip-flop is in the symmetric S state (Section II) $h = \eta^2(1-R)^2/4R^2$. If η satisfies condition (12), then $h > 1$ and, thus, the state is not stable. However, if (12) is not satisfied, then $h < 1$ and S is a stable state.

Consider now the case when the flip-flop is in one of the bistable states B (Section II), for example, state 2. h is less than one because dS_1/dS_2 is close to zero. Thus, the flip-flop is stable in state 2, provided the flip-flop parameters and external injected light permits a value of $\eta \ln(1/R)S_2$ sufficiently greater than $S_{\text{ext,thr}}$. A similar argument holds when the flip-flop is in state 1.

To ensure correct operation of the flip-flop, η should be somewhat greater than the lower bound (12). In the numerical example that we will present (Table I), η is twice the lower bound. Variations in laser parameters could cause the lower bound (12) to be higher than expected. By setting η somewhat larger than the lower bound, the flip-flop will still operate when there is some variation in the laser parameters. Furthermore, noise in the system has to cause a large change in the master laser output to cause a change of state.

If light external to the flip-flop is injected into the master laser (for example laser 2), the power injected into the slave laser decreases until it reaches approximately $S_{\text{ext,thr}}$. At this point, h becomes greater than one, making the current state (in our example state 2) unstable. A transition then occurs to the other bistable state, which is stable (in our example state 1).

To estimate the value of S_2^{ext} required to switch states, we assume that $\eta \ln(1/R)S_2 = S_{\text{ext,thr}}$ is the point at which h becomes greater than one. Furthermore, we assume that S_1 is not significant before switching occurs (if for example the flip-flop

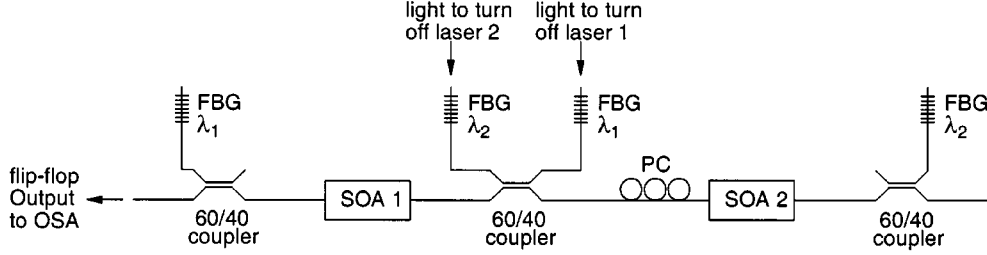


Fig. 5. Implementation of flip-flop. Each component laser is formed by a SOA and two FBGs.

is in state 2). With these assumptions, the value of S_2^{ext} required for changing states S_{sw} can be found to be

$$S_{\text{sw}} = \frac{1}{\zeta_{\text{th}}} \left(1 - \frac{1}{\eta \ln(1/R) \zeta_{\text{th}}} \right) S_{\text{st}}. \quad (17)$$

From (17), (9), and (7) we can obtain a useful expression for the power required for changing states P_{sw} , in terms of the power out of one of the facets of an isolated laser P_{st}

$$P_{\text{sw}} = \frac{2R}{1-R} \left(1 - \frac{2R}{\eta(1-R)} \right) P_{\text{st}}. \quad (18)$$

To show the steady-state behavior of the flip-flop, we numerically found the steady-state points for the full rate equation model of the flip-flop [(1) and (2)] using a fourth-order Runge–Kutta method. The steady-state points were found for various values of external injected light S_2^{ext} starting at $S_2^{\text{ext}} = 0$. S_1^{ext} was set to zero. For each value of S_2^{ext} , the state variables were found with the flip-flop initially in state 1 and also initially in state 2. The simulation parameters are given in Table I, with the semiconductor and active region parameters coming from [12].

The flip-flop action can be clearly seen when the state variables S_1 and S_2 are plotted against S_2^{ext} , (Fig. 4). If the flip-flop is initially in state 2 with laser 2 lasing, then it will remain in state 2 until S_2^{ext} reaches the level S_{thr} . Note that S_2 is reduced as S_2^{ext} is increased toward S_{thr} , while at the same time S_1 remains approximately constant and close to zero. When $S_2^{\text{ext}} = S_{\text{thr}}$, S_2 is reduced to a level such that laser 1 is no longer forced below threshold and the flip-flop abruptly changes to state 1 with laser 1 lasing.

The flip-flop will then remain in state 1 even if S_2^{ext} returns to zero. If the flip-flop is initially in state 1, then it will remain in state 1 for all values of S_2^{ext} . The flip-flop behaves in a similar way to that shown in Fig. 4 when S_2^{ext} is set to zero and S_1^{ext} is varied.

The accuracy of the estimates $S_{\text{ext,thr}}$ and S_{sw} obtained from the simplified model can be assessed by noting when switching between states occurred in the numerical example. In Fig. 4, switching occurs when S_2 is down to about 6.7×10^4 , making $\eta \ln(1/R) S_2 = 3.6 \times 10^4$. This value is close to $S_{\text{ext,thr}}$ (6% higher see Fig. 2), which has a value of 3.4×10^4 . Furthermore, from Fig. 4, switching occurs when $S_2^{\text{ext}} = 1.47 \times 10^4$, close to (about 14% less than) the predicted S_{sw} of 1.7×10^4 photons. Estimates of the switching photon number more accurate than S_{sw} may require knowledge of specific laser properties such as β and use of the full rate-equation model (1), (2). Hence, they may not be as applicable as S_{sw} .

Up to this point, it has been assumed that the gain experienced by light injected into a laser is the same as the gain for light at the lasing wavelength of the laser. However, in some situations, light injected into the laser may have a significantly different wavelength or polarization, resulting in a significant gain difference. We assume now that the injected light has a gain per unit length of $(1 + \Delta)G_i$, where Δ can be positive or negative and $\Delta \cdot G_i$ is the gain difference between injected and lasing light.

Our results on the properties of the flip-flop are based on the slope of the linear region in plots of S_i^{ext} versus S_i , like Fig. 2. We denote the new slope due to the gain difference as $-\zeta_{\text{th}\Delta}$ and it can be found from (2), (3), (4), (6), and (8) to be

$$-\zeta_{\text{th}\Delta} = \frac{(1 + \Delta)(e^{\alpha_{\text{int}} \Delta L} (1/R)^{1+\Delta} - 1)}{2L\alpha_{\text{int}} \Delta + 2(1 + \Delta) \ln(1/R)}. \quad (19)$$

Using this new value for the slope, we can find the minimum η for bistable operation and P_{sw} as was done previously.

In summary, we presented a simplified model of the flip-flop based on the steady-state laser characteristics. The simplified model provided the following. An intuitive explanation of the flip-flop operation and an estimate of the required injected light to cause a change in state (17). Furthermore, we can see that important properties, such as the conditions for bistability and the power required to change states, are primarily dependent on the controllable parameters R , η and P_{st} . However, care should be taken when applying the results as they are based only on the steady-state laser characteristics.

IV. EXPERIMENT

A. Experimental Setup

To verify the flip-flop concept and theory, we constructed two coupled lasers from: SOAs, which acted as gain sections, FBGs, which acted as wavelength-dependent mirrors, and couplers, which provided coupling (and attenuation) between the components, (Fig. 5). Laser 1 is formed from SOA 1 and the two λ_1 FBGs. Laser 2 is formed from SOA 2 and the two λ_2 FBGs. The central coupler permits coupling between the lasers. The two outside couplers ensure the reflectivities of the wavelength selective mirrors formed by the FBGs are identical on each side of a SOA. The polarization controller (PC) corrects for polarization changes in the connecting fibers. In this flip-flop, the center frequencies of the FBGs determine the wavelengths, which are $\lambda_1 = 1552.52$ and $\lambda_2 = 1558.98$ nm.

The actual cavity length of the lasers was approximately 7 m due to the fiber connections between the components. In Section

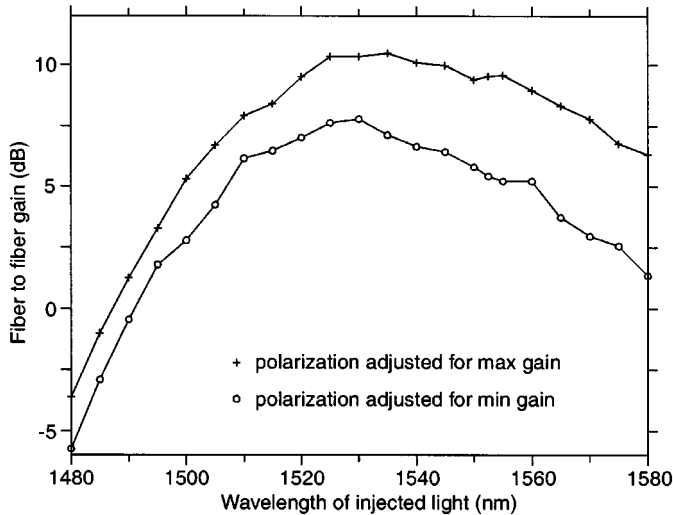


Fig. 6. Fiber-to-fiber gain characteristics of an SOA used in flip-flop. Note that the gain was measured when the SOA formed part of a laser. Hence, the carrier density and also gain were clamped at the laser threshold values.

II, we did not employ models of lasers with extended cavities as are present in the experiment. However, in this paper, we only deal with the steady-state properties of the flip-flop. In theory, there is no difference between the steady-state characteristics of the lasers and flip-flop with extended cavities and those of the system we have modeled in Section II.

The SOAs were supplied packaged and with fiber pigtailed attached. The coupling efficiency between a fiber pigtail and the SOA chip is denoted here by k . The factor k is not known exactly, but the SOA manufacturer estimates it to be 0.56 (-2.5 dB). The SOA residual facet reflectivities were less than 10^{-4} and sufficiently small so that they could be ignored. The SOAs employed a strained bulk active region and were manufactured by JDS-Uniphase.

The amplification of light through one of the SOAs (from pigtail to pigtail) while it formed part of a laser is shown in Fig. 6. From Fig. 6, it can be seen that there is a significant dependence of the gain on wavelength. However, from 1552 to 1559 nm, the gain is approximately constant. Furthermore, there is some gain dependence on the polarization of the input light. The dependence of gain on the polarization will affect the coupling requirements and switching threshold (19). This issue of polarization-dependent thresholds will be important when using optical fiber inputs, as the polarization is poorly controlled. To decrease the threshold variability will require that the gain medium used in the lasers be made polarization insensitive.

External light to change the state of the system was injected into the laser that was currently the master through one of the central FBGs.

For the flip-flop switching measurements, the injection currents for the SOAs were adjusted to give approximately equal output power for the two lasers. Laser 1 had an injection current of 121 mA, a threshold current of 107 mA, and the output power from one of the fiber pigtailed of its SOA was 1.15 mW. The same parameters for laser 2 were 108 mA, 86 mA, and 1.15 mW, respectively.

B. Measurements

In our experimental setup, we have access to the SOAs through their fiber pigtailed, and we define parameters such as reflectivity and coupling with respect to the fiber pigtailed instead of the SOA chip interface. With the new parameters, we can obtain system properties independent of the unknown coupling efficiency k . Hence, we introduce new variables R^f , η^f , and P_i^f , which are related to previously defined variables by

$$R^f = R/k^2 \quad (20)$$

$$\eta^f = \frac{\eta(1-R)}{k^2} \quad (21)$$

$$P_i^f = \frac{kP_i}{1-R} \quad (22)$$

where

R^f proportion of photons leaving the SOA pigtail that are reflected back into the pigtail (via the FBGs);

η^f proportion of photons leaving the fiber pigtail of one SOA and entering into the fiber pigtail of the other SOA;

P_i^f power at the lasing wavelength flowing out of the pigtail.

In previous sections, results were derived based on light emitted from the laser, that is, after the light has passed the laser mirror. In the experiment, the optical fields are accessed before the laser mirrors (which are the FBGs and couplers), since we measure light at the SOA fiber pigtailed. Hence, the optical power measured will be $1/(1-R)$ times that external to the laser. Thus a factor of $1-R$ occurs in (21) and (22).

R^f and η^f can be estimated from the specifications of components such as couplers and FBGs, and taking into account typical losses for the fiber connectors between the components. In our setup, the estimated values are $R^f = 0.12$ and $\eta^f = 0.52$. Assuming a value of 0.56 for k gives $R = 0.038$ and $\eta = 0.165$. Note that R , η and the ratio of injection current to threshold current are approximately the same in the experiment as in the simulation of Section III.

To verify the model of the laser with injected light given by (1) and (2), one of the lasers in the setup was set apart and injected with light. We measured the output power at the lasing wavelength from a fiber pigtail of the SOA for various amounts of light injected into a fiber pigtail of the SOA. The injected light came from a tunable laser source that was protected by an optical isolator. The wavelength and polarization of the injected light was set close to that of the lasing light, so that its gain through the SOA would be very close to the gain seen by the lasing light.

The output power from the SOA pigtail, at the lasing wavelength, versus the injected power, is plotted in Fig. 7. The shape of the curve in Fig. 7 can be seen to be qualitatively the same as that in Fig. 2. More importantly, the slope of the initial linear region of the curve can quantitatively confirm the laser model. In Section II, the slope of the linear region was given in terms of photon numbers as $-\zeta_{th}$. We measure power so we must convert the photon numbers to power values using (7) and (5). Furthermore, using (22), and noting that the power injected into the

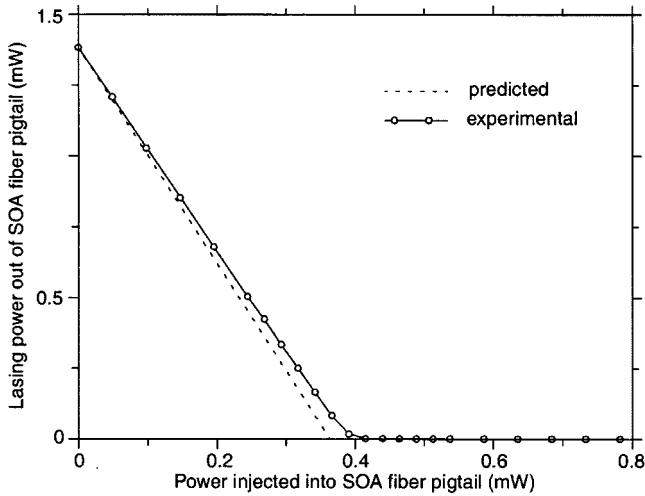


Fig. 7. Laser output power versus injected power showing predicted and experimental curves.

SOA via the pigtail has the same coupling efficiency k , we arrive at the slope of injected power versus output power

$$-\frac{k_v^2}{2R} = -\frac{1}{2R^f}, \quad (23)$$

A good estimate of R^f was found from the component characteristics. However, it can be measured precisely by realizing that when the laser is lasing, the gain of the SOA from fiber pigtail to fiber pigtail, is forced to be $1/R^f$.

We measured the value of R^f to be 0.132, by measuring the amplification of a small amount of injected light through the SOA. The slope of the linear region of Fig. 2 is approximately -3.56 , which is within a few percent of the expected value of -3.8 . Hence, in this experiment, our laser model of Section II, which in comparison to [5] includes Γ and α_{int} , predicts well the behavior of the laser with injected light.

In Section III, it was predicted that changing of the flip-flop state occurred when the level of injected light from the master into the slave laser reached S_{extthr} . To verify this prediction, we performed the following: we determined how much power was being injected into the slave laser from the master laser just before a change in state occurred. The master laser was then removed from the setup and replaced by the isolated tunable laser source. The wavelength and polarization of the light from the tunable laser source were adjusted to be the same as that of the master laser. A graph of injected power versus output power for the slave laser (Fig. 8) was obtained in the same manner as that of Fig. 7. (Note that the laser currents and, hence, output powers and S_{extthr} were different in the measurements taken for Figs. 7 and 8).

The point at which the extension of the initial linear portion of the graph crosses the x -axis is S_{extthr} , but is now expressed in injected power. The power injected into the slave just before a change in state occurred, is plotted on this graph and its relation to S_{extthr} can be seen. The point is approximately 25% higher than the value of S_{extthr} . The higher than expected value may be due to noise in the lasers, causing excursions down to S_{extthr} , and/or inaccuracies in reconstructing the effect of the master laser with the tunable laser source.

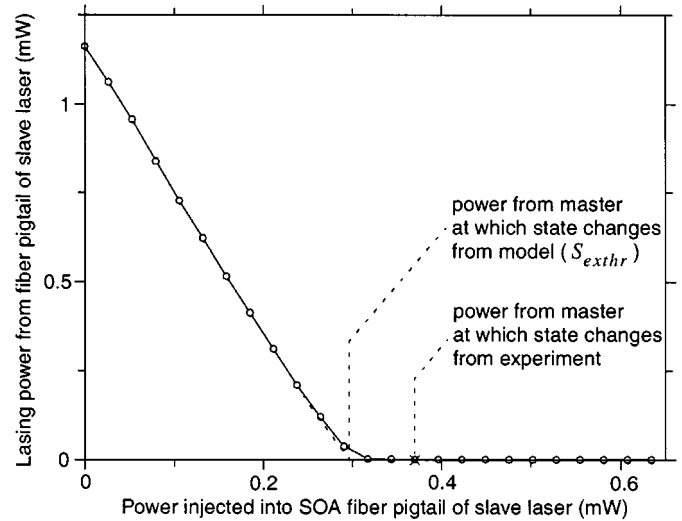


Fig. 8. Laser output power versus injected power for slave laser. Also shown is the power injected from the master laser just before a state change occurred and how this compares to the point at which a state change is assumed to occur in the model.

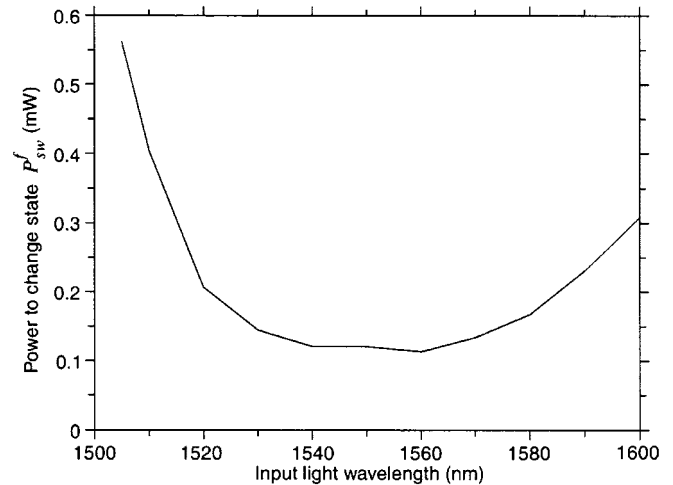


Fig. 9. Input power required to change flip-flop state versus wavelength.

Light was injected into the master from a source external to the flip-flop to reduce the power from the master and cause the change in state of the flip-flop just examined. The power that the external light source must inject into the master laser to change states was given in (18). However, as for the slope value (23), an expression for the state change power can be derived from (18), which gives the power to be injected into the SOA pigtail P_{sw}^f in terms of the lasing power out of a SOA pigtail P_{st}^f and R^f, η^f

$$P_{\text{sw}}^f = 2R^f \left(1 - \frac{2R^f}{\eta^f} \right) P_{\text{st}}^f, \quad (24)$$

We injected light from the isolated tunable laser source into the master laser (laser 1, in this case) through one of the central FBGs. The wavelength of the injected light was 1551.5 nm and its polarization was adjusted for maximum gain through SOA 1. From the experiment, the power required to change states was 0.121 mW. Equation (24) gives the estimate $P_{\text{sw}}^f = 0.149$ mW. The experimental value is 20% less than the estimate P_{sw}^f . In the simulation (Section III), the actual power to change states was

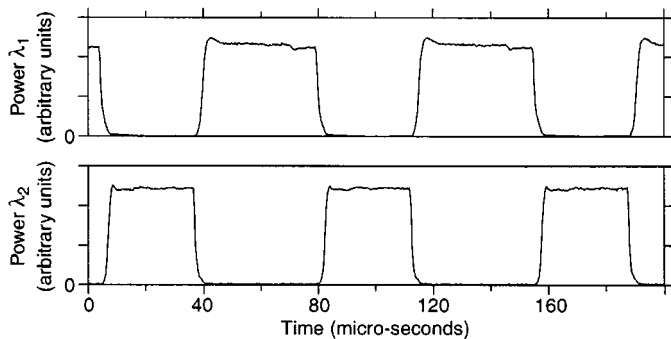


Fig. 10. Oscilloscope traces showing power at λ_1 and λ_2 . The regular toggling between states can be clearly seen.

also less than the estimate by a similar amount, 14%. (Note that P_{sw}^f is the external power injected into the flip-flop to cause a state change, whereas Fig. 8 shows the amount of power injected into the slave laser by the master just before a state change occurs.)

We were able to change the flip-flop state with light of wavelengths between 1505 and 1600 nm (excluding of course λ_1), a range of 95 nm. The power required to change the state is plotted versus wavelength in Fig. 9. Note that we were only able to test up to the tunable laser source wavelength limit of 1600 nm.

Finally, to demonstrate the flip-flop operation, we toggled the flip-flop state regularly by injecting light pulses into the laser which was master in the current state. Four microsecond-wide light pulses were generated every 75 μ s. Each pulse was split into two pulses of approximately equal magnitude. One of these pulses was injected into laser 1, while the other was delayed in a fiber delay line for 33 μ s before being injected into laser 2. The effect of the two pulses was to regularly toggle the flip-flop between its two states. In Fig. 10, oscilloscope traces of the optical powers at wavelengths λ_1 and λ_2 are shown, after optical-to-electrical conversion via photo-diodes. The switching between states can be clearly seen.

V. CONCLUSION

In this paper, a system of two lasers used to form an optical flip-flop was presented, and a static model to describe the flip-flop was developed. The flip-flop model was based on a laser model which assumed a constant carrier density along the laser length. Furthermore, it was assumed that laser and injected light experienced the same gain and losses as they travelled along the laser cavity.

From the steady-state characteristics of the laser model, how to choose controllable parameters such as laser mirror reflectivity, inter-laser coupling, and laser output power for desired operation was determined.

An experimental flip-flop was constructed using fiber Bragg gratings, SOAs, and other commercially available, fiber-based components. The results from the experiment were in good agreement with the theory developed earlier in the paper. The good agreement between theory and experiment demonstrates that the individual laser and flip-flop models are accurate.

The speed and transient switching behavior of the system were not discussed in the paper. Rather, steady-state operation

was focussed on. It is likely that the speed of the system will be dependent on the intrinsic modulation bandwidth of the individual lasers.

The implementation of the flip-flop presented here requires only gain sections (SOAs), some frequency-selective element (for example Bragg gratings), and waveguides for connecting components. Hence, the implementation of this concept could be integrated into a photonic integrated circuit.

ACKNOWLEDGMENT

The authors would like to thank the anonymous reviewers for their helpful comments on the manuscript.

REFERENCES

- [1] H. Kawaguchi, "Bistable laser diodes and their applications: State of the art," *IEEE J. Select. Topics Quantum Electron.*, vol. 3, pp. 1254–1270, Oct. 1997.
- [2] R. Lang and K. Kobayashi, "External optical feedback effects on semiconductor injection laser properties," *IEEE J. Quantum Electron.*, vol. QE-16, pp. 347–355, Mar. 1980.
- [3] G. J. Lasher and A. B. Fowler, "Mutually quenched injection lasers as bistable devices," *IBM J.*, no. 8, pp. 471–475, Sept. 1964.
- [4] J. L. Oudar and R. Kuszelewicz, "Demonstration of optical bistability with intensity-coupled high gain lasers," *Appl. Phys. Lett.*, vol. 45, pp. 831–833, Oct. 1984.
- [5] R. Kuszelewicz and J. L. Oudar, "Theoretical analysis of a new class of optical bistability due to noncoherent coupling within a twin-laser system," *IEEE J. Quantum Electron.*, vol. QE-23, pp. 411–417, Apr. 1987.
- [6] J. E. Johnson, C. L. Tang, and W. J. Grande, "Optical flip-flop based on two mode intensity bistability in a cross-coupled bistable laser diode," *Appl. Phys. Lett.*, vol. 63, pp. 3273–3275, Dec. 1993.
- [7] M. T. Hill, "All optical flip-flop based on coupled laser diodes," *Microwave and Opt. Technol. Lett.*, vol. 25, no. 3, pp. 157–159, May 2000.
- [8] M. J. Adams, J. V. Collins, and I. D. Henning, "Analysis of semiconductor laser optical amplifiers," in *Proc. Inst. Elect. Eng.*, vol. 132, Feb. 1985, pp. 58–63.
- [9] G. P. Agrawal and N. K. Dutta, *Long-Wavelength Semiconductor Lasers*. New York: Van Nostrand Reinhold, 1986.
- [10] J. J. D'Azzo and C. H. Houpis, *Linear Control System Analysis and Design Conventional and Modern*, 3rd ed. New York: McGraw-Hill, 1988.
- [11] C. S. Chang, "Analytical methods for obtaining the root locus with positive and negative gain," *IEEE Trans. Automat. Contr.*, vol. AC-10, pp. 92–94, Jan. 1965.
- [12] J. Farré, "Optical amplifiers in fiber-optic communication systems," Ph.D. dissertation, TFL Telecommun. Res. Lab., Horsholm, Denmark, Appendix A, Feb. 1993.

Martin T. Hill (S'96–A'97), photograph and biography not available at the time of publication.

H. de Waardt, photograph and biography not available at the time of publication.

G. D. Khoe (S'71–M'71–SM'85–F'91), photograph and biography not available at the time of publication.

H. J. S. Dorren, photograph and biography not available at the time of publication.